The Kinetics of σ-Phase Precipitation in AISI 310 and AISI 316 Steels

JAN BARCIK

The kinetics of σ-phase precipitation in AISI 310 and AISI 316 steels were studied. An attempt was made to express the rate of precipitation of σ-phase with formal kinetic theory equations. It was established that rate of precipitation of σ-phase is a function of temperature that agrees with the Johnson-Mehl equation.

I. INTRODUCTION

It was established by Morley and Kirkby[1] that the kinetics of σ-phase precipitation are dependent not only on annealing conditions but also on the chemical composition and structure of the austenitic steel. In the opinion of these authors the σ-phase precipitates more slowly when directly formed from the austenite than during precipitation through the ferrite. Blenkinsop and Nutting[2] postulated that the process of σ-phase precipitation follows the TTT_i curves. These curves were first prepared for σ-phase precipitating from cast steel of type 25 pct Cr-20 pct Ni, containing 0.22 pct carbon.[3] Similar TTT_i curves for σ-phase forming in type AISI 316 steel are given in Reference 4.

The object of the present studies was to describe the kinetics of σ-phase formation in chromium-nickel austenitic steels using formulae of formal kinetic theory and to determine the factors governing the rate of precipitation of this phase.

II. TEST MATERIALS

Tests were conducted on type AISI 310 austenitic steels with varying contents of carbon and silicon and also on AISI 316 steel stabilized with titanium (Table I). Solutionizing of these steels in the conditions laid down in Polish Standards did not achieve total solution of the carbides (Table II). The presence of carbides in the solutionized steel is primarily due to the high carbon content, exceeding solubility in the chromium-nickel austenite. Raising of solutionizing temperature applied to steel AISI 314 gave a slight reduction in quantity of undissolved carbide $M_{23}C_6$ (from 1.5 pct to 1.2 pct by weight) at the same time causing increased size of the austenite grains.

After solutionizing, AISI 316 Ti steel contained, as well as undissolved titanium interstitial phases, also σ-ferrite in a quantity estimated on the basis of magnetic measurements at 1.8 pct. All the solutionized steels were next subjected to isothermal annealing in the temperature range from 873 to 1173 K every 50 K, for a time of up to 10,000 hours.[5,6] The quantity of σ-phase precipitated during this long-lasting annealing of the steel was determined using the method of selective electrolytic extraction.[7]

Isolation of phases precipitated in austenite during long lasting annealing of the steel was carried out for two different electrolytes (Table III). In electrolyte I all excess phases were extracted simultaneously while in electrolyte II the carbides only were extracted and the σ-phase was dissolved. The quantity of σ-phase was calculated from the difference in quantities of isolates obtained in the two electrolytes.

The phase composition of the isolates was determined by the X-ray phase analysis method. X-ray diffraction patterns were obtained by the powder method using cameras of diameter 114.6 mm and CoK_α radiation. Phase identification was based on the ASTM tables.

III. RESULTS AND DISCUSSION

A. *Rate of σ-Phase Precipitation*

The values of σ-phase content, determined by the method of selective electrolytic extraction, provided the data for plotting the kinetic curves representing the quantity of phase precipitated as a function of isothermal time of steel annealing. From these curves were prepared the TTT_i curves for σ-phase precipitating in the type 310 steels (Figure 1). The differences to be observed between these curves (Figures 1(a), (b), and (c)) indicate that the kinetics of σ-phase precipitation depend on the presence of $M_{23}C_6$ carbide undissolved during the solutionizing process. The size of the austenite grains also exerts a marked influence on the progress of σ-phase formation. In steels with a carbon content of the order of 0.14 pct (AISI 310 and AISI 314 steels), this phase precipitates most rapidly at temperature 1073 K. The minimum time required for σ-phase to record at this temperature is three hours for AISI 310 steel and four hours for AISI 314 steel. The slower rate of formation of σ-phase in steel AISI 314 is due to the larger grain size of the austenite in this steel than in AISI 310.

In the first stage of the precipitation process the σ-phase nucleated on the interphase boundary between $M_{23}C_6$ not dissolved during steel saturation and the austenite (Figure 2). In steel AISI 310 S the σ-phase precipitated in trace quantities and very slowly. This may be presumed to be due to the total solution of carbide $M_{23}C_6$ during solutioning of this steel. The minimum time required for the σ-phase to appear in this steel is about 100 hours.

A similar TTT_i curve was obtained for σ-phase precipitating in AISI 316 steel stabilized with titanium (Figure 3). The temperature at which the σ-phase precipitates most rapidly is 1073 K, and the minimum time to observe the presence of this phase is 20 hours. This time is almost 75 times briefer than that needed for the σ-phase to appear in nonstabilized AISI 316 steel.[4] This observed difference

---

JAN BARCIK is with Silesian University, Institute of Physics and Chemistry of Metals, 12, Bankowa 40-007 Katowice, Poland.

Manuscript submitted October 29, 1981.

Table I. Chemical Composition of the Tested Steels

AISI Type	Content of Alloying Elements, Wt Pct								
	C	Mn	Si	P	S	Cr	Ni	Mo	Ti
310 S	0.03	1.08	0.35	0.032	0.028	24.34	22.27	—	—
310	0.135	1.38	0.60	0.035	0.022	24.34	19.50	—	—
314	0.14	0.54	2.20	0.018	0.013	24.21	19.70	—	—
316 Ti	0.07	1.60	1.04	0.031	0.018	16.84	12.45	2.48	0.48

Table II. Solutionizing Conditions, Content, and Type of Undissolved Carbides

AISI Type	Solutioning Conditions			Carbides Content Wt Pct	Phase Composition of Undissolved Carbides (X-Ray Identification)
	T K	t Hours	Quenchant		
310 S	1393	0.5	water	0	—
310	1393	0.5	water	1.2	$M_{23}C_6$
314	1393	0.5	water	1.5	$M_{23}C_6$
	1493	0.25	water	1.2	$M_{23}C_6$
316 Ti	1523	0.5	water	0.6	TiC, TiN, Ti_2S

Table III. Conditions of Electrolytic Extraction of Phases

Electrolyte Number	Electrolyte Composition	Electrolysis Conditions			Isolate Phase Composition
		T K	mA/ cm^2	t Hours	
I	5 g $C_2H_2O_4$ + 200 cm^3 HCl	290	50	2	carbides and
			5	12	α-phase
II	10 pct vol HCl + 90 pct vol C_2H_5OH	290	5	24	carbides

in the speed with which the σ-phase appears is due to the different mode of precipitation. In the stabilized steel this phase precipitates *via* the ferrite (α-phase) arising as a result of destabilizing of the austenite during precipitation of the TiC carbide (Figure 4),[8] whereas in the nonstabilized AISI 316 steel the σ-phase nucleates directly in the austenite and on the $M_{23}C_6$ carbide and χ-phase.[4,9] The $\gamma \rightarrow \alpha$ phase transformation is accompanied by nonuniform division of the alloying elements between the austenite and the ferrite. The ferrite, enriched with chromium and other ferrite-forming elements, is more susceptible to precipitation of σ-phase than the austenite; furthermore, the diffusion rate in the ferrite is almost one hundred times greater than in the austenite.

The curves in Figures 1 and 3 show the logarithmic function of precipitation rate against temperature. This relation may be expressed by the following analytical equation:[10,11]

$$J = A(T)[\exp - (\Delta G^* + Q)/kT] \qquad [1]$$

where J is the precipitation rate, $A(T)$ is a constant depending on temperature of annealing of the steel, ΔG^* is the change in free energy due to formation of a nucleus, Q is the activation energy of the σ-phase precipitation process, k is the Boltzmann constant, and T is the absolute temperature. The coefficient before the exponent is only slightly dependent on temperature, as compared with the exponential function. This makes it possible to assume that $A(T)$ has a constant value in a given temperature interval. At temperatures lower than that at which the σ-phase precipitates at the highest rate, the value of ΔG^* is very small and may be neglected in calculations. Hence, the rate of σ-phase precipitation represented in the lower ends of the "C" curves in Figures 1 and 3 may be written as:

$$J = A \exp -\left(\frac{Q}{kT}\right) \qquad [2]$$

$$\text{or, } \ln J = \ln A - \frac{Q}{kT} \qquad [2a]$$

Results obtained confirm the linear relationship between the natural logarithm of rate of precipitation and the reciprocal of annealing temperature (Figure 5). The degree of fitting of experimental results to a straight line is represented as a coefficient of linear regression as in Eq. [2a] (see Table IV).

The fact that the straight lines in Figure 5 are not parallel indicates that rate of σ-phase precipitation depends on the

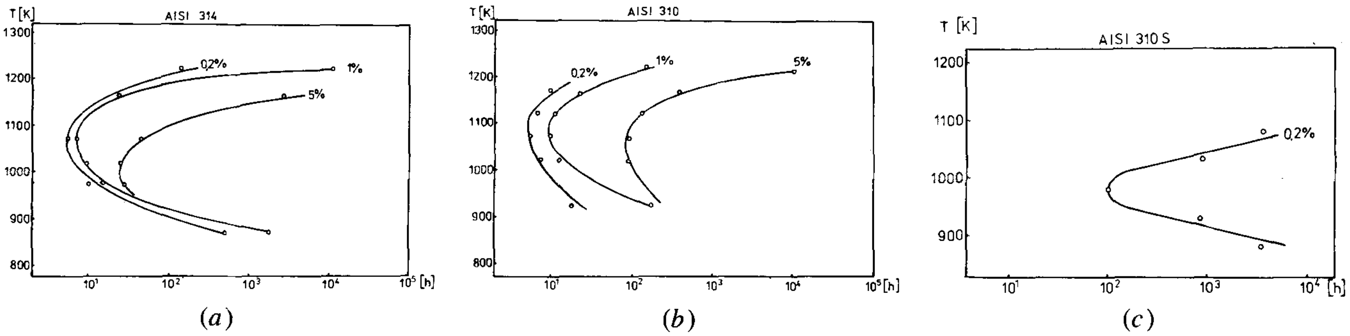

(*a*) (*b*) (*c*)

Fig. 1—*TTT*, curves for σ-phase precipitating in steels: (*a*) AISI 314, (*b*) AISI 310, (*c*) AISI 310S.

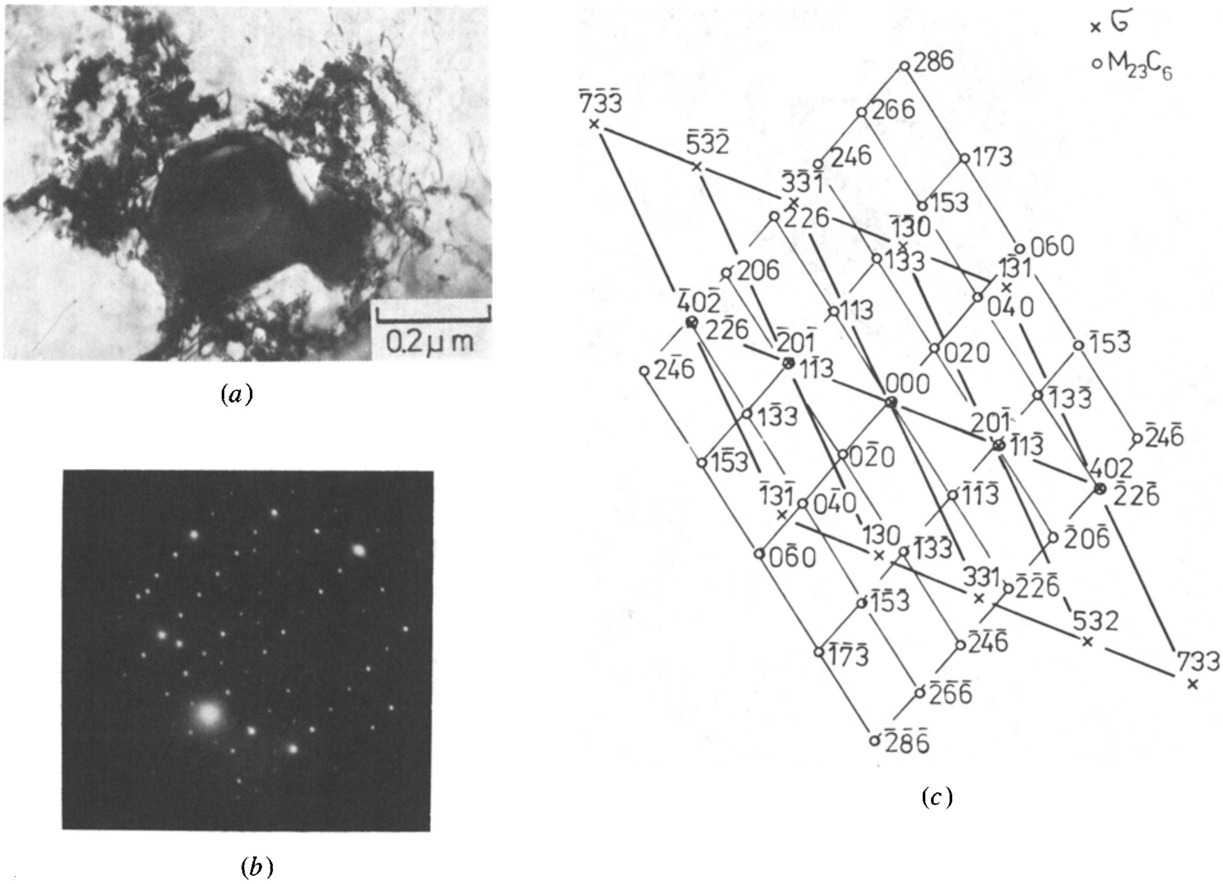

(*a*)

(*b*)

(*c*)

Fig. 2—σ-phase grain on the primary boundary of carbide $M_{23}C_6$ particles in AISI 314 steel annealed for 1000 h at 873 K. (*a*) Picture in bright field of view, (*b*) electron diffraction pattern from (a), and (*c*) σ-phase and $M_{23}C_6$ carbide diagram with indices marked.

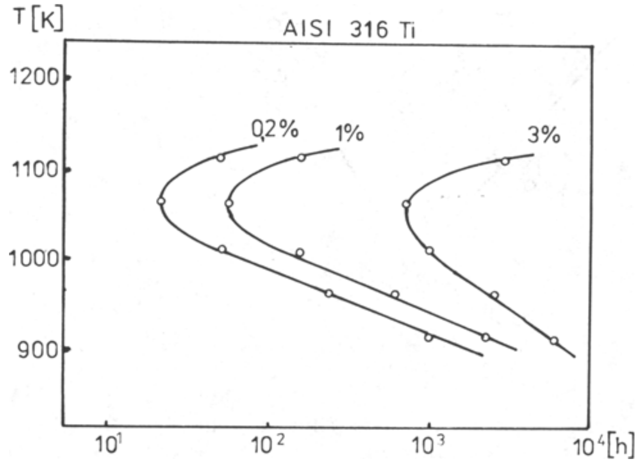

Fig. 3—*TTT*, curve for σ-phase precipitating in AISI 316 steel stabilized with titanium.

time of annealing. In the initial stage of the process the σ-phase precipitates on the boundaries of the austenite grains. The activation energy of this type of σ-phase nucleation is principally determined by diffusion at the boundaries of the austenite grains and at the austenite/$M_{23}C_6$ carbide interface. In further stages of the process the σ-phase nucleates inside the austenite grains. Thus, the precipitation rate and also the activation energy of the process are dependent on the volumetric diffusion within the austenite grains.

The tangent of the angle of inclination of the straight lines to the abscissa (the 1/T axis) is equal to the ratio of activation energy to the Boltzmann constant. Calculated from this ratio the activation energy has a mean value of 167 kJ/mol for steels of type AISI 310 S, 310, and 314 following short time annealing, while after long time annealing (more than 100 hours) this value is 234 kJ/mol. These values carry a large error as the precision of determination of σ-phase content in the steel was low (± 0.2 pct), hence the values of activation energy obtained are not very accurate. Nevertheless, these values are close to the energy of chromium diffusion in the austenite. The energy of chromium diffusion in the austenite is independent of its chemical composition and has a value of 191 kJ/mol for diffusion over the boundaries of the austenite grains, and 243 kJ/mol for volumetric diffusion.[12] Thus, the determined values of the process activation energy reflect the method of nucleation of the σ-phase.

The activation energy of the process of σ-phase precipitation in AISI 316 Ti steel is about 178 kJ/mol. This energy is the result of the energy of diffusion of chromium and molybdenum in the ferrite.

The rate of nucleation of the equilibrium phases in a supersaturated solid solution during isothermal annealing may be described by the Johnson-Mehl equation:[10,13,14]

$$Z = A\left[1 - \exp - \left(\frac{t}{\tau}\right)^n\right] \qquad [3]$$

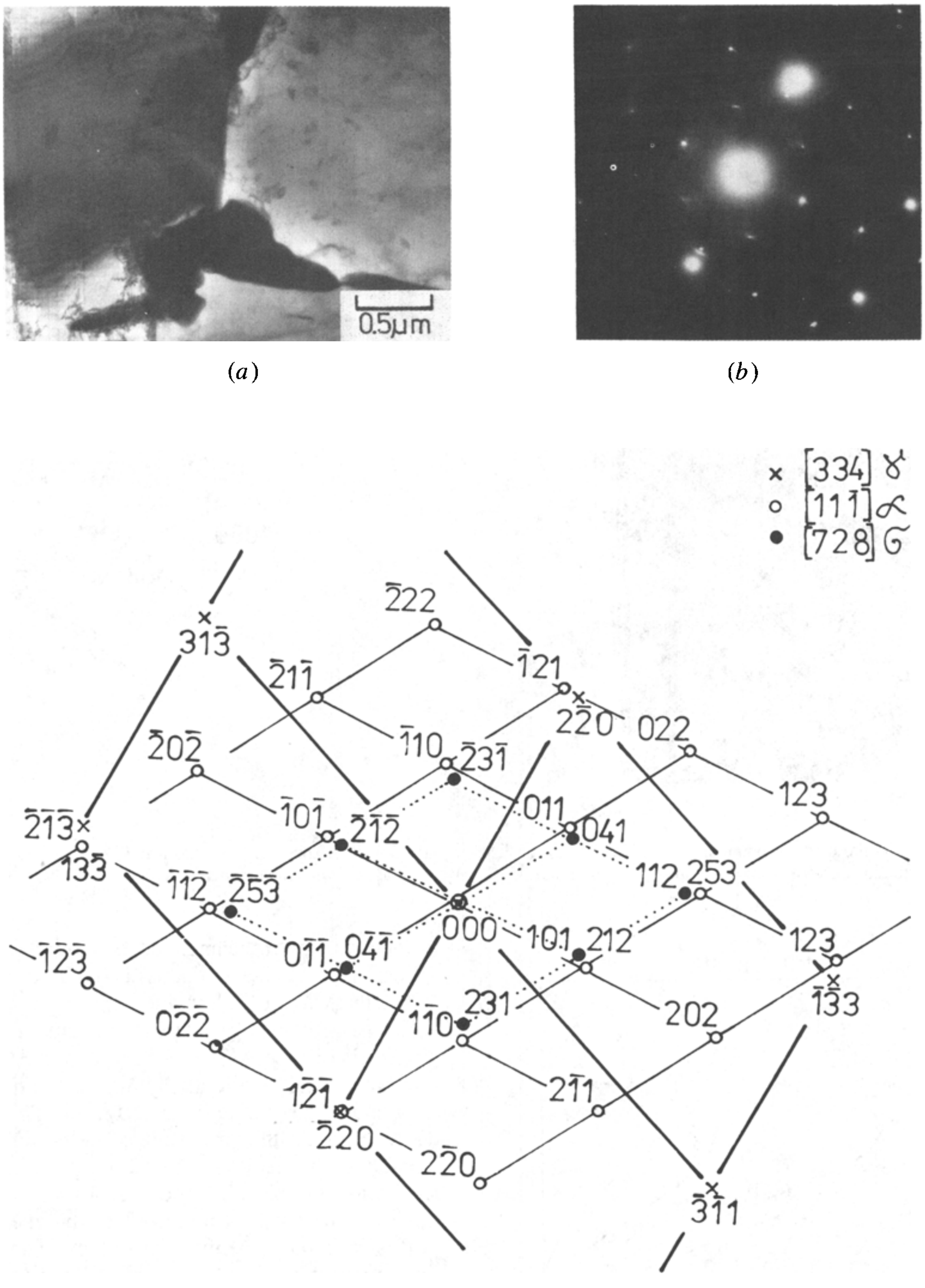

(*a*) (*b*)

(*c*)

Fig. 4—Structure of AISI 316 Ti steel after annealing for 3000 h at 1023 K. (*a*) Microscope picture, (*b*) electron diffraction pattern, and (*c*) ferrite and austenite σ-phase diagram with indices marked.

where Z is the quantity of equilibrium phase precipitated in isothermal annealing time t; A is the maximum quantity of σ-phase which can precipitate in the given alloy; τ is the shortest time required to reach equilibrium between σ-phase and the steel matrix, dependent on distance between precipitated particles and on diffusion coefficient; and n is the form factor. When transformed, Eq. [3] becomes

$$\log\left[\ln\left(\frac{1}{1-W}\right)\right] = n \log t - n \log \tau \qquad [4]$$

where $W = Z/A$. The graph of function $\log[\ln(1/(1-W))]$ *vs* $\log t$ is a straight line if the precipitation rate agrees with the Johnson-Mehl equation.

The rate of σ-phase precipitation during isothermal annealing is governed by Eq. [4](Figure 6). The degree of fitting of experimental results to the theoretical straight line described in Eq. [4] is expressed by a coefficient of linear regression correlation (Table V). Table V also gives the values of form factor n and constant τ.

The fact that the straight lines in Figure 6 are not parallel and also variations exist in form factor n calculated by the

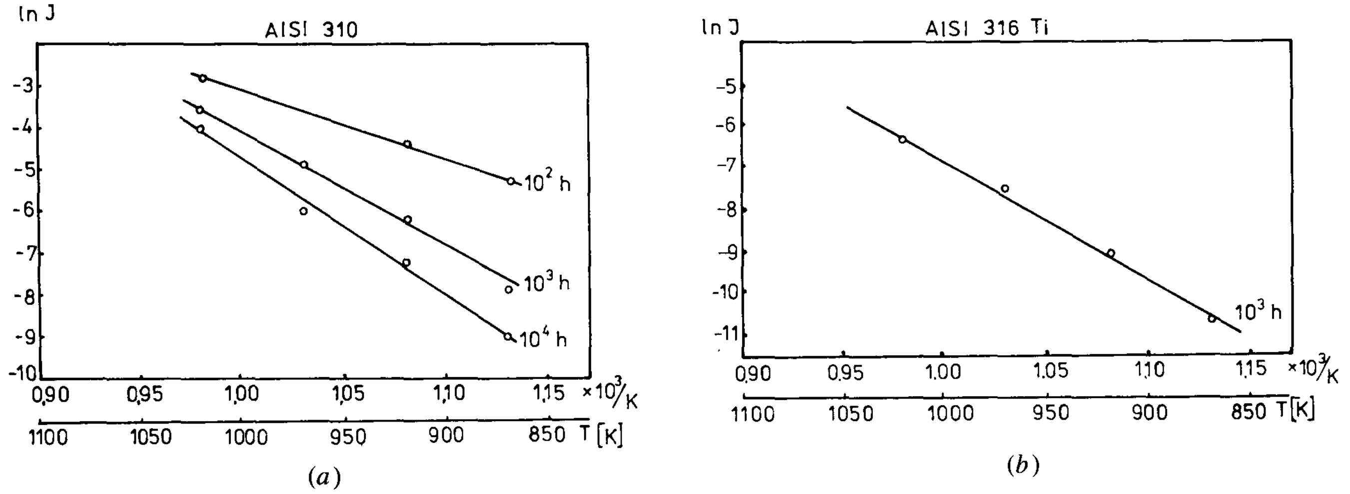

Fig. 5—Rate of σ-phase precipitation as a function of temperature in a specific time: (*a*) AISI 310, (*b*) AISI 316 Ti.

Table IV. Degree of Matching of Experimental Results to the Linear Relationship in Equation [2a]

Annealing Time, Hours	For Steels	
	AISI 310	AISI 316
100	0.98	—
1000	0.96	0.96
10000	0.97	—

method of least squares, considered in conjunction with the observed nucleation points and the shape of the σ-phase grains, confirms the correctness of the Cahn theory of the location of nucleation.[10,15] Transmission electron microscope observations of thin foils showed that short time annealing of AISI 310 steel at temperatures 873 to 923 K leads to nucleation of σ-phase on the boundaries of the austenite grains. These nuclei grow and develop in the form of an oval "pond" (Figure 7).

On the other hand, long time annealing causes precipitation of σ-phase in the form of plates within the austenite grains. The deflection of lines log $[\ln(1/(1 - W))]$ *vs* log t for these temperatures confirms the microscope observations. Raising the annealing temperature from 973 to 1073 K leads to simultaneous nucleation of σ-phase on the boundaries and within the austenite grains. From this it may be concluded that the rate of σ-phase precipitation is governed by nucleation rate and not by speed of growth. The growing particles take the form of plates for which the habit plane is one of the octahedral planes of the austenite. At temperatures above 1023 K, coagulation of the earlier precipitated σ-phase particles takes place simultaneously with the precipitation process. According to the formal theory of the kinetics of phase changes developed by Cahn and Ham,[15,16] the form factor n for particles nucleating on the grain boundaries should be about 0.25 to 0.5, while for particles nucleating on the dislocations inside the grains of the matrix, n should have a value of 0.75 to 1. From consideration of differences in values of form factor n for steels AISI 310 and AISI 316 stabilized with titanium it may be concluded that the kinetics of σ-phase precipitation are markedly dependent on the rate of molybdenum diffusion. Increase in

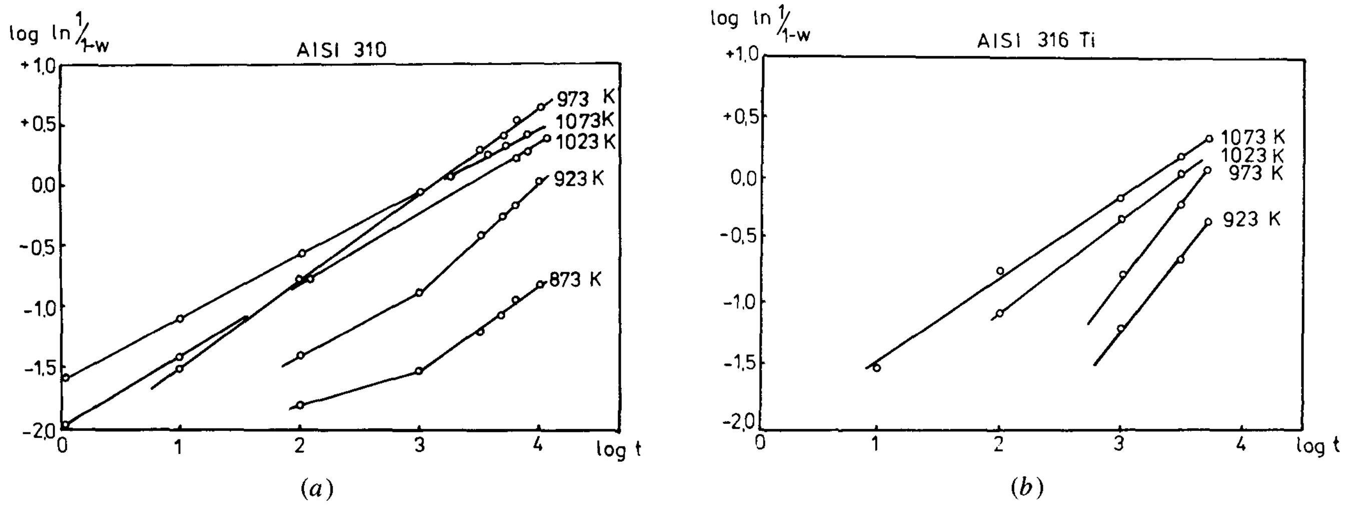

Fig. 6—Rate of σ-phase precipitation as a function of time of isothermal annealing: (*a*) AISI 310, (*b*) AISI 316 Ti.

Table V. Coefficient of Linear Regression Correlation, Form Factor n and Constant τ

Temperature of Annealing, K	For AISI 310 Correlation Coefficient	n	τ, Hours	For AISI 316 Ti Correlation Coefficient	n	τ, Hours
873	0.99	0.51	—	—	—	—
	0.98	0.81	$2.88 \cdot 10^6$			
923	0.99	0.49	—	0.99	1.2	$1.01 \cdot 10^4$
	0.98	0.84	$7.9 \cdot 10^3$			
973	0.99	0.72	$1.2 \cdot 10^3$	0.99	1.1	$0.65 \cdot 10^4$
1023	0.99	0.79	$0.72 \cdot 10^3$	0.99	0.75	$0.28 \cdot 10^4$
1073	0.99	0.75	$0.96 \cdot 10^3$	0.98	0.54	$0.19 \cdot 10^4$

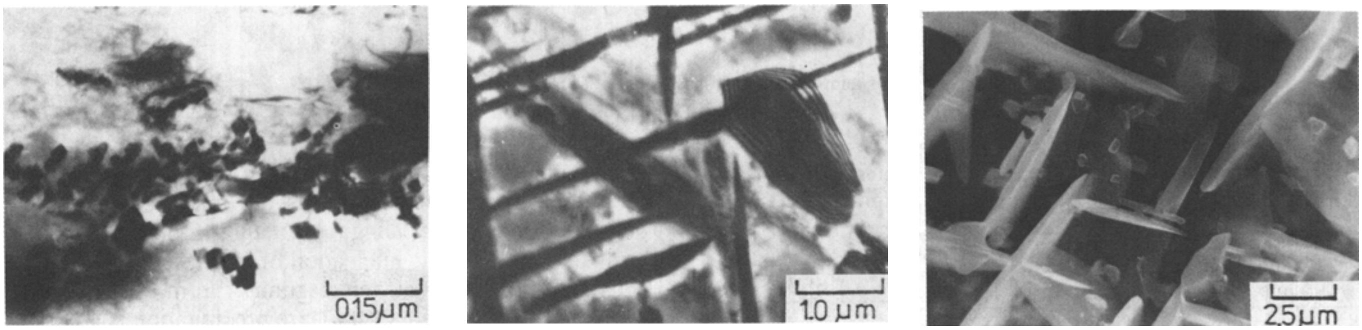

(*a*) (*b*) (*c*)

Fig. 7 — Shape and distribution of σ-phase precipitating in nonstabilized AISI 310 austenitic steels: (*a*) precipitation on the grain boundaries during annealing of the steel at 600 K, (*b*) σ-phase precipitation throughout the whole austenite volume, and (*c*) distribution of σ-phase plates precipitated inside the austenite grains — picture by reflected electrons of a deep etched polished microsection.

the rate of molybdenum diffusion decreases the slope of the straight lines log $[\ln(1/(1 - W))]$ *vs* log t.

B. *The Influence of Certain Factors on Rate of σ-Phase Precipitation*

The existence of a relationship between rate of σ-phase precipitation and size of austenite grains was postulated by Pryce *et al.*[17] In these studies the influence of solutionizing the temperature on the process of precipitation of this phase in type 310 steel was examined. The steel was solutionized in two different sets of conditions (Table II). Solutionizing at 1493 K caused growth of the austenite grains together with a slight lowering of the content of nondissolved $M_{23}C_6$ carbide in comparison with solutionizing at 1393 K. Annealing at 1073 K showed that precipitation of the σ-phase takes place more rapidly in fine-grained steel than in coarse-grained (Figure 8). This slower progress of the precipitation process in coarse-grained steel is presumably associated with the smaller number of "advantageous" places for nucleation of the σ-phase due to reduction of the total surface of grain boundaries.

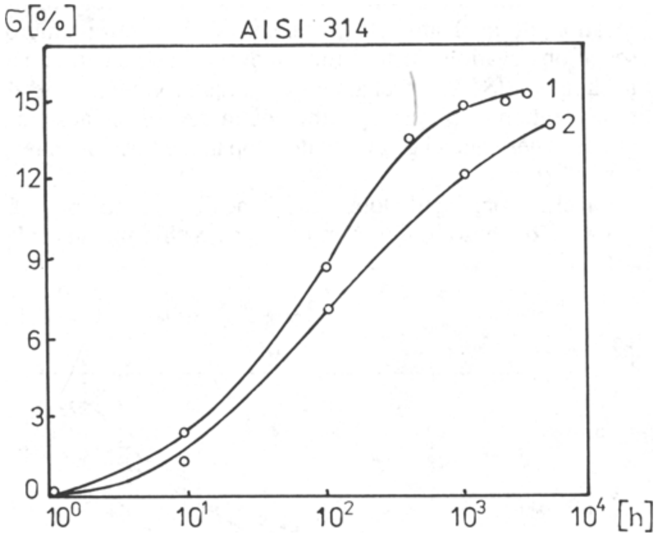

Fig. 8 — Quantity of σ-phase precipitated in AISI 314 steel as a function of time of isothermal annealing at temperature 873 K after solutionizing at temperatures: 1 — 1393 K, 2 — 1493 K.

The effect of plastic deformation on the process of the σ-phase precipitation in austenitic steels has been the subject of considerable research efforts; however, results obtained did not allow a definitive opinion to be formulated. Certain authors postulate that plastic deformation, insufficient to initiate recrystallization, inhibits the progress of σ-phase precipitation.[18] However, when this deformation causes the transformation $\gamma \rightarrow \alpha$, this accelerates the precipitation of the σ-phase.[2,19,20] Results reported in References 21, 22, and 23 suggest that, independent of its magnitude, plastic deformation promotes nucleation of the σ-phase. The process of precipitation of this phase during creep has been studied here. It was established that stresses not exceeding the creep time boundary do not cause σ-phase precipitation in steels not susceptible to formation of this phase. In cast steels HK-40 and HK-40 stabilized with niobium, the presence of σ-phase was not detected after 42,000 hours work at a temperature of 1053 K under a pressure of 3.0 to 3.5 MPa.[24] On the other hand, creep in steels susceptible to σ-phase precipitation, *e.g.*, steels type 310, 314, and 316 accelerates precipitation of the σ-phase and widens the temperature of occurrence of this phase in comparison with annealing without loading. For example, during isothermal annealing of 314 steel, the σ-phase does not appear until after 1000 hours at 873 K, while during creep the presence of this phase in the steel was ascertained after 1000 hours at 773 K.

IV. CONCLUSIONS

1. The kinetics of σ-phase precipitation are governed by rate of diffusion of chromium and other sigma-forming elements and also by nucleation mode. The precipitation progress is described by the Arrhenius law, *i.e.*, $J = K \exp - (\Delta G^X + Q)/\mathrm{k}T$, where activation energy of the process is equal to the diffusion energy of alloy elements in the austenite.
2. Precipitation of σ-phase during isothermal annealing follows the Johnson-Mehl law, *i.e.*,

$$\log\left[\ln\left(\frac{1}{1-W}\right)\right] = n \log t - n \log \tau$$

   In agreement with the theories of Cahn and Ham, the form factor n reflects the location of nucleation.
3. The rate of precipitation of σ-phase through the ferrite is more rapid by almost two orders of magnitude than the corresponding rate of precipitation directly from the austenite.
4. The solutioning conditions influence the kinetics of σ-phase precipitation due to growth of the austenite grains. In coarse-grained steels the σ-phase is precipitated more slowly than in fine-grained.
5. The presence of $M_{23}C_6$ carbides not dissolved during the process of solutionizing accelerates nucleation of σ-phase.

REFERENCES

1. J. J. Morley and H. W. Kirkby: *J. Iron Steel Inst.*, 1952, vol. 172, p. 129.
2. A. P. Blenkinsop and J. Nutting: *J. Iron Steel Inst.*, 1967, vol. 205, p. 953.
3. R. Blower and G. J. Cox: *J. Iron Steel Inst.*, 1970, vol. 208, p. 769.
4. B. Weiss and R. Stickler: *Metall. Trans.*, 1972, vol. 3, p. 851.
5. J. Barcik: *The sigma phase precipitation process in chromium-nickel austenitic steels,* publisher: Silesian Univ., Katowice, 1979, p. 136.
6. J. Barcik: *Archiw. Nauki o Materialach,* 1981, vol. 2, p. 63.
7. J. Barcik and D. Fyda: *Prace Chemiczne IV,* publisher: Silesian Univ., Katowice, 1974, p. 61.
8. J. Barcik: *Hutnik,* to be published.
9. M. Blicharski, P. Korgul, and S. Gorczyca: *Archiw. Hutn.*, 1978, vol. 23, p. 303.
10. J. W. Christian: *The Theory of Transformations in Metals and Alloys,* Pergamon Press, Oxford, 1965, pp. 471-95.
11. J. N. Habstetter: *Decomposition of austenite by diffusion process,* V. F. Zackay and M. J. Arronson, eds., J. Wiley, New York, NY, 1962, p. 1.
12. A. F. Smith: *Met. Sc.*, 1975, vol. 9, pp. 181, 375, 425.
13. J. S. Kirkby: Ref. 11, p. 39.
14. J. K. L. Lai Meshkat: *Met. Sc.*, 1978, vol. 12, p. 415.
15. J. W. Christian: in *Physical Metallurgy,* R. W. Cahn, ed., Chapter X, North-Holland Co., Amsterdam, 1965.
16. F. S. Ham: *J. Appl. Phys.*, 1959, vol. 30, pp. 915, 1518.
17. L. Pryce: *J. Iron & Steel Inst.*, 1956, vol. 178, p. 289.
18. M. Blicharski, P. Korgul, and S. Gorczyca: *Proc. of IV Conf. on Electron Microscopy of the Solid State,* organized by the Metallurgy Committee of Polish Academy of Sciences, S. Gorczyca, ed., publisher: Institute of Ferrous Metallurgy, Gliwice, 1975, p. 199.
19. J. Eysymontt and J. Widerman: *Proc. of III Conf. on Electron Microscopy of the Solid State,* organized by the Metallurgy Committee of Polish Academy of Sciences (held at Kraków-Bartkowa), 1973, publisher: SITPH Katowice, 1973, p. 75.
20. J. N. Calvet and P. Petreguin: *Mem. Sc. Rev. Metallur.*, 1974, vol. 71, p. 591.
21. M. Blicharski: *Hutnik,* 1977, vol. 44, p. 581.
22. P. Duhaj, *et al*: *J. Iron Steel Inst.*, 1968, vol. 206, p. 1245.
23. J. E. Spuriell, *et al*: *Metall. Trans.*, 1973, vol. 4, p. 1533.
24. Z. Bojarski and J. Barcik: *Hutnik,* 1977, vol. 44, p. 331.